IN-SITU RESONANCE RAMAN MEASUREMENTS OF A HYBRID ELECTROCHROMIC CELL WITH A GEL REDOX (I_3^-/I^-) ELECTROLYTE

Angela Šurca Vuk, Boris Orel,*

National Institute of Chemistry, Hajdrihova 19, SI–1000 Ljubljana, Slovenia

Philippe Colomban

LADIR UMR 7075 CNRS & Paris VI University, 2 Rue Henry Dunant, 94320 Thiais, France

Received 11-09-2003

Abstract

A hybrid electrochromic (HEC) device was constructed from optically active nanocrystalline WO_3 film and transparent platinised SnO_2:F-glass electrodes encapsulating a gel redox electrolyte. The electrolyte was prepared from an organic-inorganic ICS-PPG precursor that was synthesized from bis end-capped triethoxy silane and poly(propyleneglycol)-bis-(2-amino-propyl)ether (MW = 4000). KI and I_2 in a molar ratio KI:I_2 = 10:1 were a source of an I_3^-/I^- redox pair while valeric acid was used as a catalyst for the solvolysis reactions of the ICS-PPG precursor. The stability and kinetics of colouring/bleaching changes of the HEC device were determined by using in-situ UV-visible spectroelectrochemical measurements between +2 and –2 V (CV, CC).

In-situ micro-Raman spectroscopic technique was used to follow the functioning of the HEC device. The excitation line of 647.1 nm was focused in the redox electrolyte, closer to the platinised SnO_2:F-glass electrode and the resonance Raman spectra were recorded during the cyclovoltammetric scanning of the potential between +2 and –2 V. The resonance Raman spectra were dominated by the symmetric $\nu_s(I_3^-)$ stretching of I_3^- ions at 111 cm^{-1}. Its relative intensity changes revealed the course of the redox reaction $3I^- \leftrightarrow I_3^- + 2e^-$ in the electrolyte and were accompanied by the intensity changes of the background Rayleigh scattering. The latter were assigned to the dissociation/association of the KI microcrystallites in the gel redox electrolyte during the intercalation and deintercalation of K^+ ions in electrochromic WO_3 film.

Introduction

Conventional – battery type[1,2] – EC devices with two films with intercalation properties are well established as "smart windows",[2,3] enabling the control of heat-loads and the illumination levels inside the buildings simply by the application of the potential pulse at the will of the occupant. The battery-type EC device consists of two optically transparent and electronically conducting (TCO) electrodes supporting active films with intercalation properties. One film possesses electrochromic properties (usually WO_3) and colours under cathodic voltage and intercalation of Li^+ ions due to the redox reaction of

$W^{6+} + e^- \rightarrow W^{5+}$. After the opposite voltage is applied, Li^+ ions moved from WO_3 to counter-electrode film which should remain optically passive (V/Ti-oxide, $M^{III}VO_4$, M = Ce, In, Fe,…)[2,3] or should colour complementary (Ni-oxide, Ir-oxide,…).[2,4] The space between both electrodes is filled with an electrolyte containing H^+, Li^+ or other small cations in a solvent, polymer matrix (laminated design) or thin film (all-film design).[1] Such EC devices exhibit an extended open-circuit memory since the electrolyte is electronically non-conducting.

Beside the battery-like also a solution-type and a hybrid-type of EC devices exist, having in common that a constantly applied voltage is needed to retain the coloured state (self-erasing devices). The chromophore-based devices,[5] for example, with the chromophore dissolved in solution or deposited in polymeric form on TCO electrode have the colouring/bleaching times in the range of seconds or less. As a support for the redox chromophore recently also TiO_2 film was used.[6,7] Typical examples of molecular redox chromophores are viologens, conducting polymers,[8] metallopolymers and some metallophthalacyanines.[9] The construction of a hybrid EC device was recently reported by Lin et al.[10] They used Prussian blue as an electrochromically active film in contact with the heptyl viologen (V^+) dissolved in aqueous electrolyte.

The first aim of the present study was the preparation of a hybrid EC device consisting of a nanocrystalline WO_3 film[11] as an optically active film and a gel redox electrolyte containing I_3^-/I^- redox pair (Figure 1).[12,13] A platinized SnO_2:F-glass served as a counter-electrode. In this device the change from the optically transparent to the absorbing state is achieved by the simultaneous insertion of electrons and cations into optically active WO_3 film as in standard battery-type EC devices. However, the charge entering the WO_3 is compensated by the redox reaction $3I^- \rightarrow I_3^- + 2e^-$ at the Pt-electrode. Bleaching is achieved by the application of an opposite voltage: cations leave the structure of the WO_3 film and enter the electrolyte, in which at Pt electrode I^- are formed again. Hybrid-type EC devices, that do not need a counter-electrode with intercalation properties for their functioning, represent a step-forward in simplicity of EC device design. The number of active layers is diminished compared to the standard battery-type EC devices and the colouring/bleaching speeds are increased. Due to the latter property and the self-erasing effect, the hybrid EC devices are more suitable for the rear-view EC mirrors for cars than for “smart windows”.

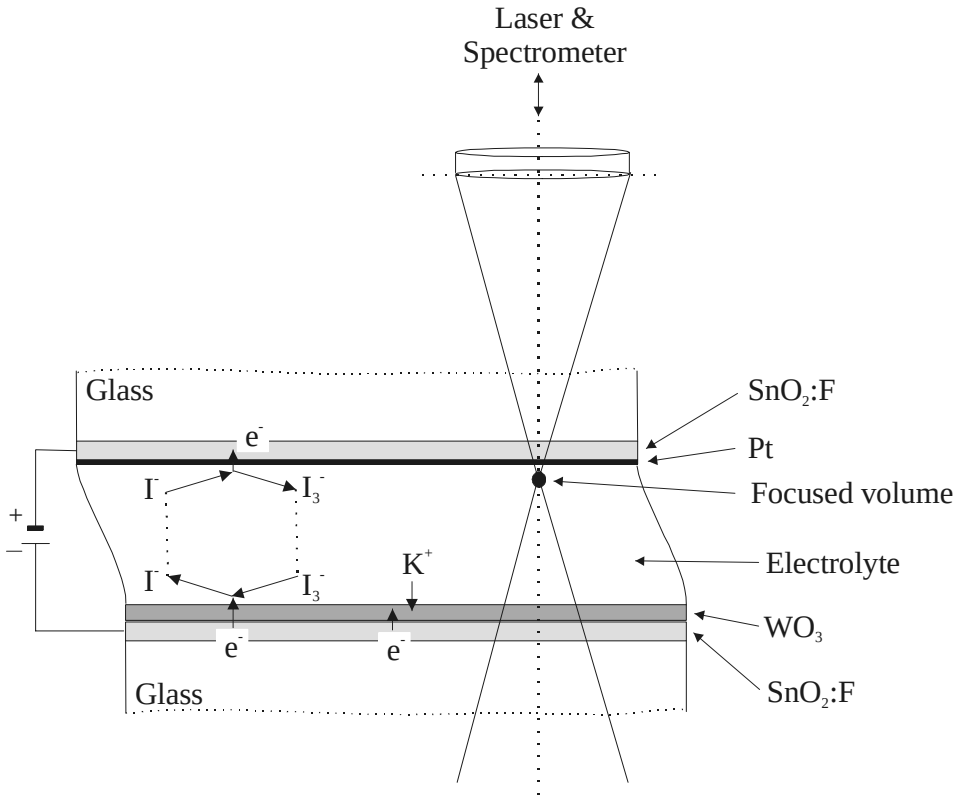

Figure 1. Schematic representation of a hybrid EC cell and in-situ resonance Raman measurements.

In the hybrid EC devices we used a gel redox electrolyte that we developed during our investigations of dye-sensitised photoelectrochemical (Grätzel) cells.[14-16] We used a Class II organic-inorganic hybrid[17] based on bis-end-capped triethoxysilane covalently bonded via urea bridges to poly(alkyleneoxide) chains (ICS-PPG). Instead of the more ionophilic and commonly used poly(ethyleneglycol)[18] we used poly(propyleneglycol) (PPG) with the molar weight of 4000. Recently, we prepared ICS-PPG containing KI and I_2, gelled it with acetic acid and used it as a redox gel I_3^-/I^- electrolyte in dye-sensitised photoelectrochemical (DS PEC) cell[14-16,19] giving an efficiency of 4–5%. This value is lower than the efficiency of DS PEC cells employing liquid redox electrolytes (~10%), but is the highest reported up to date for the semi-solid DS PECs. In this paper we present the properties of a hybrid EC device in which the gel I_3^-/I^- redox electrolyte was catalysed by valeric instead of acetic acid. The electrochemical properties were assessed by in-situ UV-visible spectroelectrochemical techniques and calculation of photopic transmittances.

The second main aim of this study was to obtain a better insight into the functioning of the hybrid EC device by in-situ resonance Raman measurements. This technique exploits the strong resonance Raman effect of I_3^- ions and is therefore a suitable tool to follow the course of the redox reaction $3I^- \leftrightarrow I_3^- + 2e^-$ in the space between two electrodes. The micro-Raman technique was already used to study the interactions of I_3^- ions with a ruthenium bipyridyl dye attached to TiO_2 film in a DS PEC cell[20] and also to study the $3I^- \leftrightarrow I_3^- + 2e^-$ process in DS PECs under open- and short-circuit conditions.[14-16] In this study we focused the laser excitation line (413.1 and 647.1 nm) on the redox electrolyte in the hybrid EC device and collected the spectra during its cyclovoltammetric cycling. From these experimental data, by following the changes in the relative intensity of the symmetric $\nu_s(I_3^-)$ stretching of I_3^- ions, we inferred how the intercalation and deintercalation from the WO_3 film influenced the course of the redox reaction $3I^- \leftrightarrow I_3^- + 2e^-$. Apart to $\nu_s(I_3^-)$ mode intensity changes we observed also the variation in the background Rayleigh scattering with potential that we ascribed to a reversible dissociation/association of the KI microcrystallites of submicrometre dimensions.

Experimental

Optically active WO_3 films were nanocrystaline with the grain size of 30 nm and were prepared by using peroxo sol-gel route.[11] A drop of the redox electrolyte was placed on the WO_3 film and immediately covered with the platinised SnO_2:F glass substrate. The redox electrolyte was prepared from organic-inorganic silicon precursor ICS-PPG that was synthesised from 3-isocyanatopropyltriethoxy silane (ICS) and poly(propyleneglycol)-bis-2-amino-propyl)ether (PPG) with a molar weight of 4000 g mol^{-1}. ICS-PPG was first dissolved in ethanol (EtOH), then KI and I_2 were added in molar ratio $KI:I_2 = 10:1$. Finally, the valeric acid ($CH_3(CH_2)_3COOH$; VaOH for short) was added as a catalyst for the gelation of ICS-PPG via aprotic solvolysis reactions.[21,22] The final product was a sol-gel network with incorporated I_3^-/I^- redox pairs, K^+ ions, some residual EtOH and ester of valeric acid as a side product of the solvolysis reactions. The redox electrolytes did not gel when kept refrigerated (4 °C).

In-situ UV-visible spectroelectrochemical measurements of the hybrid EC cells were made using the HP 8453 diode-array spectrophotometer in combination with an

EG&G PAR model 273 potentiostat-galvanostat. The cyclovoltammetric (CV) curves were obtained by the scan rate of 20 mV s^{-1} and were scanned from 0 V to –2 V, reversed to 2 V and then finished at 0 V. The kinetics of the coloration and bleaching was obtained by applying a chronocoulometric (CC) technique by performing the intercalation of K^+ ions at –2 V for 100 s and deintercalation at 2 V (100 s). Reported potentials correspond to the potential applied to the WO_3 film (working electrode) with respect to the platinised SnO_2:F-glass substrate (counter-electrode). Due to the presence of I_3^-/I^- couple in the electrolyte may the platinised counter electrode function as a quasy reference electrode with a definite constant potential according to the actual activity of the redox I_3^-/I^- pair close its surface. The potentials of working and counter electrode are not know exactly. This problem can be solved with the use of the micro-reference electrode incorporated in the electrolyte between both electrodes and this work is under progress. In addition, it might be assumed that the potential shifts of the counter electrode in the HEC cell may influence the background changes in the in-situ Raman spectra since the KI microcrystallite formation depends on potential. However, such an effect should be small compared to reactions KI (microcrystallites) $\leftrightarrow KI_{1-x} + xK^+ + xI^-$ and $I_3^- + 2e^- \leftrightarrow 3I^-$ occurring in the measured part of the electrolyte.

Prior to resonance Raman spectra measurements of ICS-PPG/EtOH/KI/I_2/VaOH sols EtOH solvent was partly evaporated in a rotary evaporator. The Raman spectra were then recorded by the excitation lines of 413.1 and 647.1 nm on two different XY DILOR spectrographs. For the measurement of the HEC cells with the 647.1 nm line the spectrograph was equipped with mixed Ar-Kr ion plasma. The HEC cell was positioned under the laser beam in such a way that the WO_3 film was on the bottom and platinised SnO_2:F on the top (Figure 1). The laser beam was then focused on the electrolyte closer to the Pt-covered counter-electrode. For in-situ resonance Raman measurements we used HEC devices that were 50 μm thick.

Results and discussion

In-situ UV-visible spectroelectrochemical characterisation

The colouring/bleaching changes of the hybrid EC device with the redox electrolyte catalysed with VaOH are shown in Figure 2. The spectra revealed that the optical change is lower than 30% for wavelengths below 500 nm, while it can even

exceed 50% at higher wavelengths. The cross-section of the optical modulation at λ = 634 nm (Figure 2C) revealed that colouring is slower (~20 s) then bleaching (5 s) for this HEC device. Optical response can be expressed also in term of a photopic transmittance T_{vis}:[23] The calculation of the photopic transmittance showed that its values were 35.0%, 31.2% and 28.9% after 10 s, 20 s and 100 s of colouring, respectively, confirming that the device coloured mostly during the first 20 s of the experiment. After bleaching the photopic transmittance achieved was 69.1.

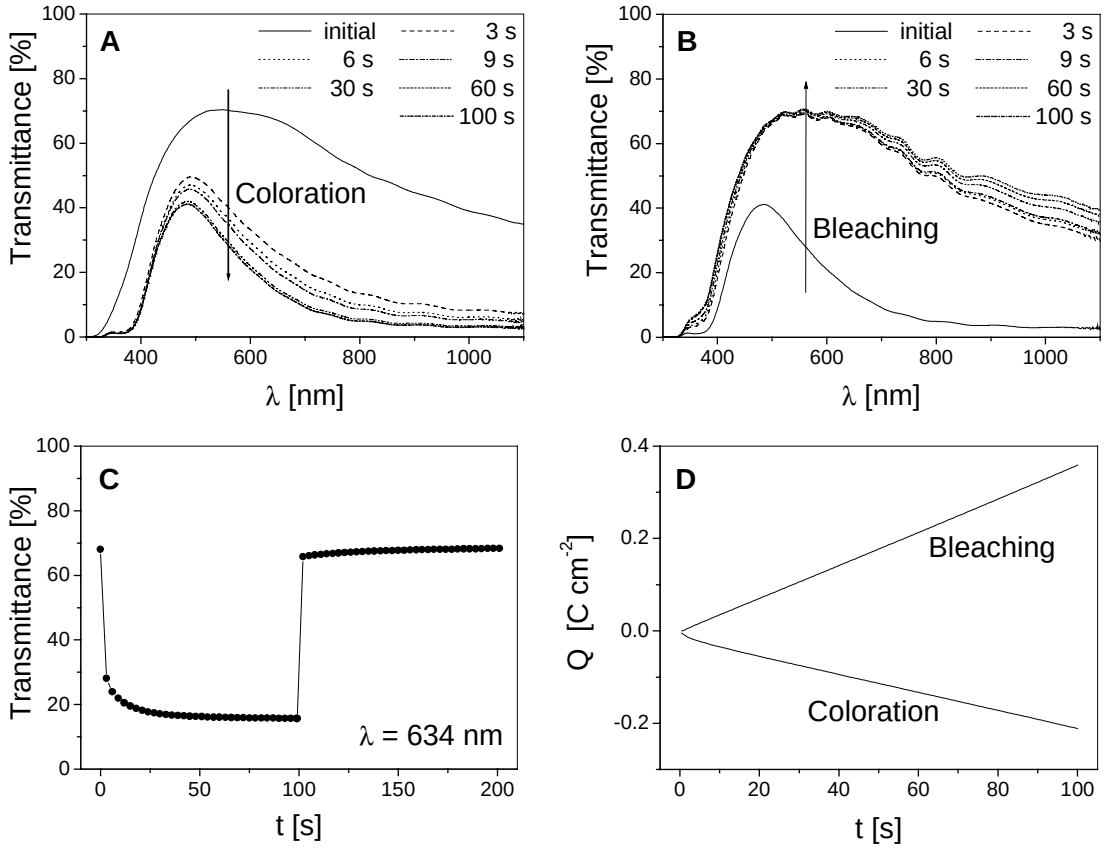

Figure 2. In-situ UV-visible spectroelectrochemical measurements of a hybrid EC cell with the electrolyte catalysed with the VaOH acid during chronocoulometric colouring/bleaching: A) spectra during colouring, B) spectra during bleaching, C) monochromatic transmittance at 634 nm and D) chronocoulometric curves.

The interesting feature of the chronocoulometric experiment is the linear response of the charge vs. time curves (Figure 2D). For the usual battery-type EC device with two films with intercalation properties is the characteristic CC response the saturation

plateau due to the limited ion-storage of the intercalation electrodes.[2,3]. The linear CC curves of HEC cells, however, do not reflect only the intercalation/deintercalation of K^+ ions in WO_3 film but also the fact that the redox reaction $3I^- \leftrightarrow I_3^- + 2e^-$ may occur at either Pt-covered or WO_3 electrode (Figure 1). Therefore, by taking 20 s as the most appropriate time for the evaluation of the electrochromic efficiency, this becomes 6.3 $cm^2\ C^{-1}$.

The intrinsic property of the hybrid EC devices is the self-erasing effect. For the HEC with VaOH it is demonstrated in Figure 3. The device was first charged at –2 V for 100 s and then disconnected from the electrical contacts. The UV-visible spectra were recorded every 3 s during the first 1000 s of the measurement, later every 600 s. It is clearly visible that most of the bleaching at λ = 634 nm occurred by 1000 s.

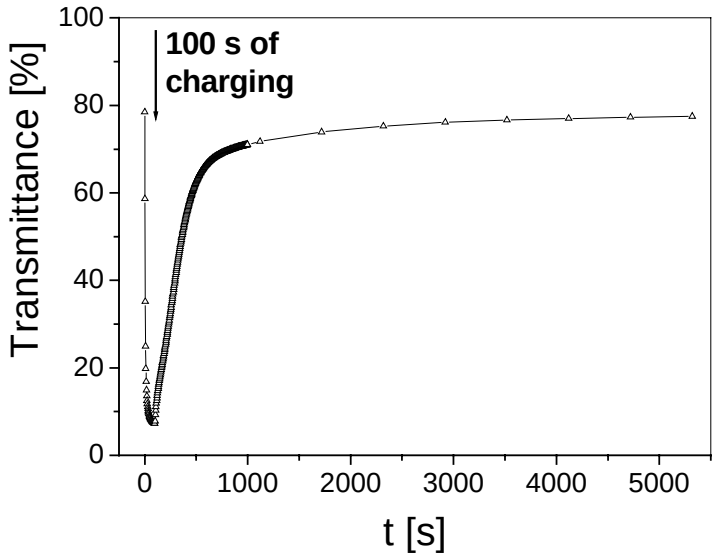

Figure 3. Self-erasing properties of a hybrid EC cell with the electrolyte catalysed with VaOH acid: the cell was charged at –2.0 V for 100 s and then disconnected from electrical contact. Monochromatic transmittance changes were followed at 634 nm.

Cyclovoltammetric (CV) curves are shown in Figure 4 together with the monochromatic transmittance response at 634 nm. When a scan rate of 20 mV s^{-1} was used the current peaks of intercalation and deintercalation of K^+ ions in WO_3 film could not be discerned (Figure 4A). They can be observed, however, between –1 and –2 V (intercalation) and in a reverse scan between 0 and 1 V (deintercalation) when either a thicker layer of the electrolyte or a longer time aged electrolyte is used in the HEC

device (see section on in-situ Raman measurements). In contrast, the CV curves in Figure 4A revealed an increase in current density at approximately –0.3 V and simultaneously the device began to colour (Figure 4B). The maximal coloration is achieved between –2 and –1.5 V in a reverse scan, while beyond this potential the transmittance started to increase to an initial value that was reached up to 2 V. The current density at –2 V decreased with the number of cycles. Stability of this device was tested up to 1210 cycle and is represented with photopic transmittances in Figure 5. It is clearly visible that the photopic transmittances in the bleached state were approximately 68% throughout the whole cycling, while the values in the coloured state varied between 30 to 40%.

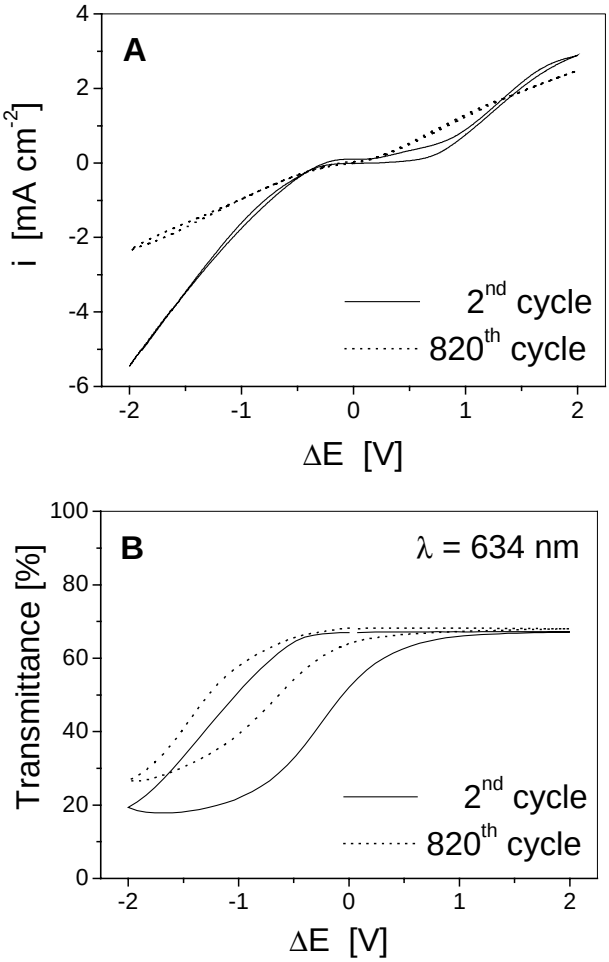

Figure 4. In-situ UV-visible spectroelectrochemical measurements of a hybrid EC cell: A) CV curves and B) monochromatic transmittance at 634 nm. The scan rate used was 20 mV s^{-1}.

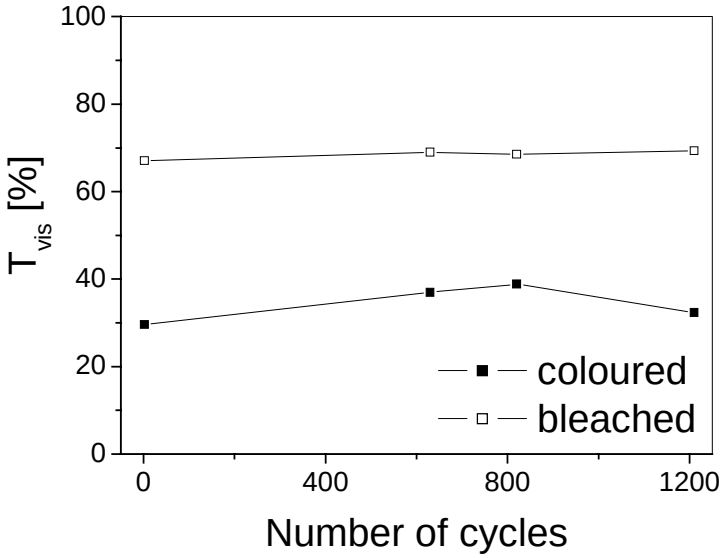

Figure 5. Photopic transmittance of a hybrid EC device in a coloured and bleached state during CV cycling with a scan rate of 20 mV s^{-1}.

Resonance Raman spectra of sols

Resonance Raman spectra of an ICS-PPG/EtOH/KI/I_2/VaOH (partly evaporated EtOH) sol were measured by the excitation lines of 413.1 and 647.1 nm (Figure 6). Positions of both excitation lines are marked on UV-visible reflection-absorption spectrum of the ICS-PPG/EtOH/KI/I_2 gel showing the two absorptions of I_3^- at 290 and 360 nm and absorption of I^- ions at 225 nm.[24,25] During our investigation of sols and gels having various KI:I_2 molar ratios we found out that for the functioning of the HEC devices the ratio of the I_3^- and I^- UV-visible absorptions should tend towards one.

In the Raman spectra recorded with either of the excitation lines we observed the symmetric ($\nu_s(I_3^-)$) stretching of I_3^- ions at 111 cm^{-1} as the dominating band and its asymmetric ($\nu_a(I_3^-)$) counterpart at 139 cm^{-1}.[12-16,25-28] In addition, in the spectrum recorded with 413.1 nm line higher harmonics at 222, 336, 452 cm^{-1}, … of the symmetric $\nu_s(I_3^-)$ mode at 111 cm^{-1} can be observed. This is due to the strengthening of the resonance Raman effect[26,27] because this excitation line lies closer to the maximum of the genuine absorption of I_3^- ions at 360 nm than the 647.1 nm line (Figure 7). The reason for the comparable intensities of the 111 cm^{-1} band in both Raman spectra (Figure 6) is the longer time of excitation and higher power used for measurements with the 647.1 nm line (180 s, 20 W) than for 413.1 nm line (35 s, 15 W), although should be –

according to the theory of the resonance Raman[26,27] – the 111 cm^{-1} significantly more intensive when measured with 413.1 nm line.

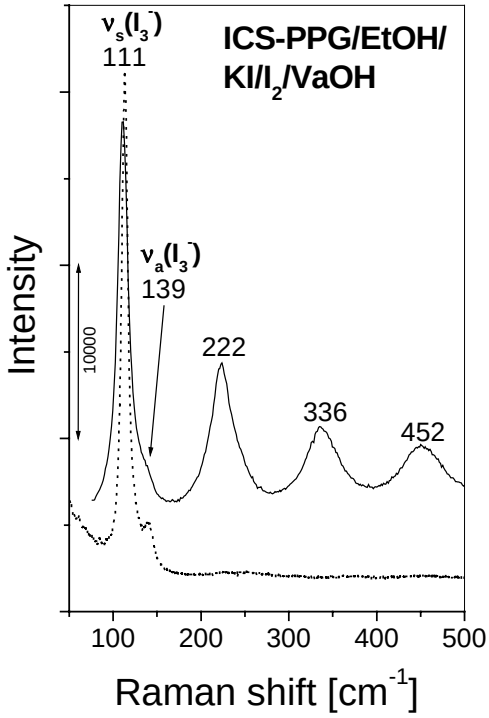

Figure 6. Resonance Raman spectra of an ICS-PPG/EtOH/KI/I_2/VaOH (EtOH partly evaporated prior to measurement) sol measured by the excitation lines 413.1 and 647.1 nm. Time of collection was 35 s at 413.1 nm and 180 s at 647.1 nm.

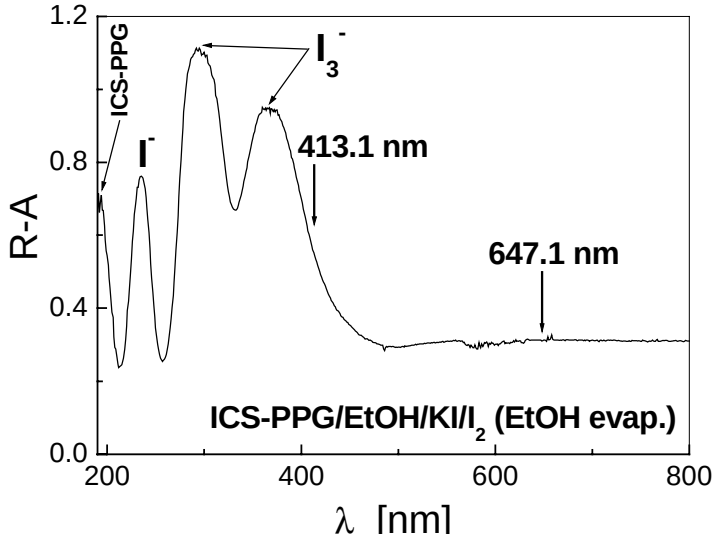

Figure 7. UV-visible reflection-absorption spectrum of an ICS-PPG/EtOH/KI/I_2 (EtOH partly evaporated prior to measurement) redox electrolyte with indicated excitation lines of 413 and 647.1 nm.

In the resonance Raman spectrum measured with the 647.1 nm excitation line the overtones between 150 and 500 cm^{-1} were not visible (Figure 6). This spectrum is dominated by an intense symmetric $\nu_s(I_3^-)$ stretching at 111 cm^{-1} and therefore suitable to obtain information about the course of the redox reaction $3I^- \leftrightarrow I_3^- + 2e^-$ in the electrolyte between the WO_3 and platinised SnO_2:F-glass electrodes in a HEC device.

In-situ resonance Raman spectra of a hybrid EC device

A schematic presentation of the in-situ resonance Raman measurements of the hybrid EC devices is depicted in Figure 1. The spectra were measured by focusing laser radiation (λ = 647.1 nm) through the SnO_2:F glass substrate and sputtered Pt layer on the redox gel electrolyte encapsulated in the HEC device. In order to follow the redox reaction that occurred in the electrolyte closer to the Pt counter-electrode, thicker EC devices than usual (~10 μm) were prepared (~50 μm).

The results of the in-situ resonance Raman measurement of the 12^{th} cyclovoltammetric (CV) potential scan of a hybrid EC device are shown in Figure 8. The CV was performed with a scan rate of 20 mV s^{-1}, starting from 0 V to –2 V, then reversed to 2 V and finished at 0 V (Figure 8A). Raman spectra, dominated with the symmetric $\nu_s(I_3^-)$ stretching at 111 cm^{-1} (Figure 11B), were measured every 50 s for a duration of 30 s, as depicted with arrows in Figure 8A. Two main features were noted in the corresponding in-situ resonance Raman spectra: (i) the absolute and relative intensity of the I_3^- mode at 111 cm^{-1} changed with potential, and (ii) the background scattering averaged over the range 200 – 500 cm^{-1} varied with potential as well. At cathodic potentials the intensity of 111 cm^{-1} band changed in the opposite direction than the background (Figure 8B,C).

The absolute integral intensity of the 111 cm^{-1} mode increased during cathodic potentials (-1 and –2 V in Figure 8C), attained minimal values at –1 V in a reverse scan and then increased again at anodic potentials. However, due to the high background intensity compared to the intensity of the $\nu_s(I_3^-)$ stretching and its pronounced changes during the CV measurement, the absolute integral intensity of $\nu_s(I_3^-)$ could not give an exact insight into the reactions taking place in the HEC cell. Therefore, the relative intensity of the 111 cm^{-1} band corrected for the intensity of the background (Figure 8C) was calculated, and this varied according to expectations. During cathodic potentials

when K^+ ions intercalated in the WO_3 film the redox reaction $3I^- \rightarrow I_3^- + 2e^-$ took place at the Pt counter-electrode, leading to an increase in the relative intensity of 111 cm^{-1} band (-2 V in Figure 8C). Due to the applied potential, the reverse reaction ($I_3^- + 2e^- \rightarrow 3I^-$) could take place in addition to K^+ intercalation at the WO_3 side of the HEC cell. Expectedly, the minimal relative integral intensity of the 111 cm^{-1} band was reached at 0 V in a reverse scan. At anodic potentials its intensity remained approximately the same (2 V in Figure 8C).

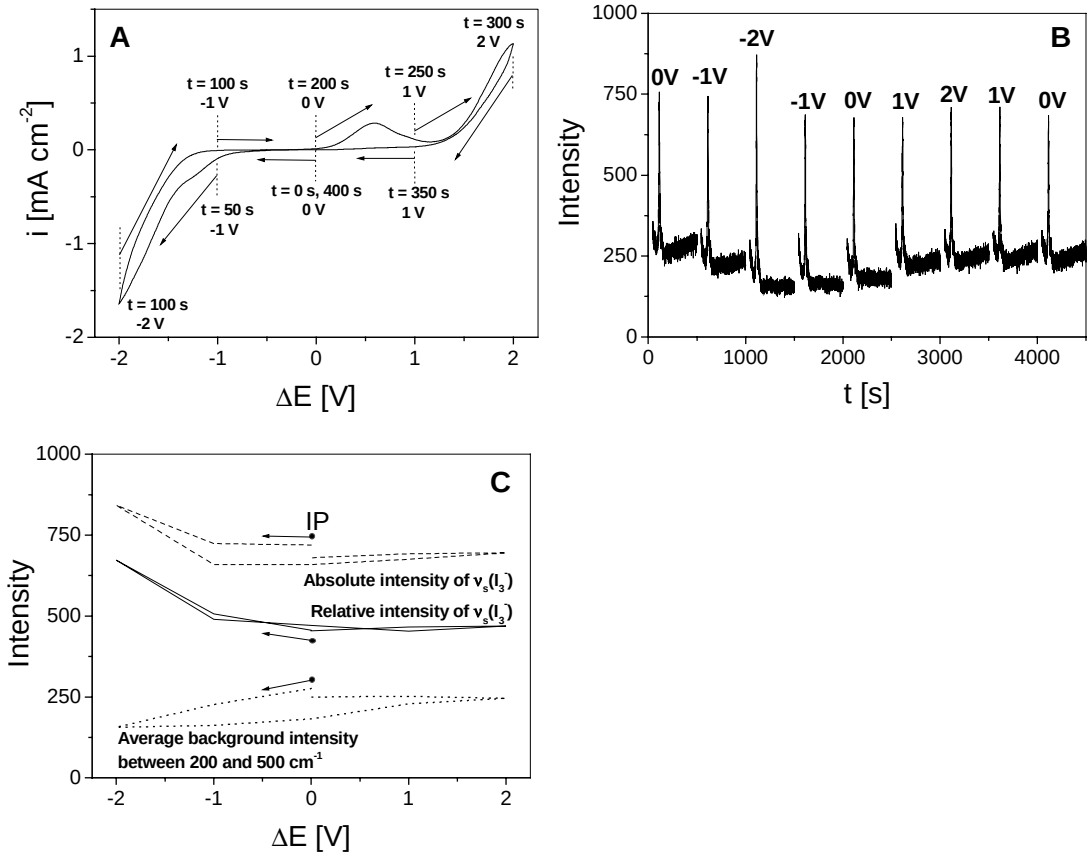

Figure 8. In-situ resonance Raman measurements (λ = 647.1 nm) of a hybrid EC cell with electrolyte catalysed with VaOH: A) CV curve (12^{th} cycle; 20 mV s^{-1}), B) all measured in-situ Raman spectra between 50 to 500 cm^{-1} and C) intensity changes of the $\nu_s(I_3^-)$ stretching band and the background. In CV curve the arrows denote the starting potential and the duration (30 s) of the Raman measurement.

The background intensity averaged over the range 200 – 500 cm^{-1} had at cathodic potentials the opposite behaviour than the relative intensity of 111 cm^{-1} mode: its intensity decreased from 0 V to –2 V then remained the same up to 0 V in a reverse scan. Beyond 0 V the intensity of the background increased again, but did not reach the initial

value. Such a variation of the background scattering intensity (Figure 8B,C) was noted also for the HEC devices in which the electrolyte was catalysed by acetic acid[12,13] and in in-situ resonance Raman spectra of the electrolyte encapsulated in DS PEC cells.[14-16] In analogy with the interpretation of the latter spectra we assumed that also in HEC devices the background intensity changes occurred due to the reaction KI (microcrystallites) $\leftrightarrow$ $KI_{1-x} + xK^+ + I^-$. Namely, because of the relatively high amount of KI and I_2 in the ICS-PPG/EtOH/KI/I_2/VaOH redox electrolyte we found out that after gelation and evaporation of EtOH part of the K^+ and I^- in the electrolyte already existed in the form of KI microcrystallites having submicrometer dimensions. The appearance of the crystalline or amorphous KX precipitates (X = Cl^-, ClO_4^-, I^-, NO_2^-) is already mentioned in the literature[29] and was found in siloxane-polyoxypropylene (PPO) hybrids doped with KI, $KClO_4$ and KNO_2. In this case the existence of crystallites was proved by X-ray diffraction.

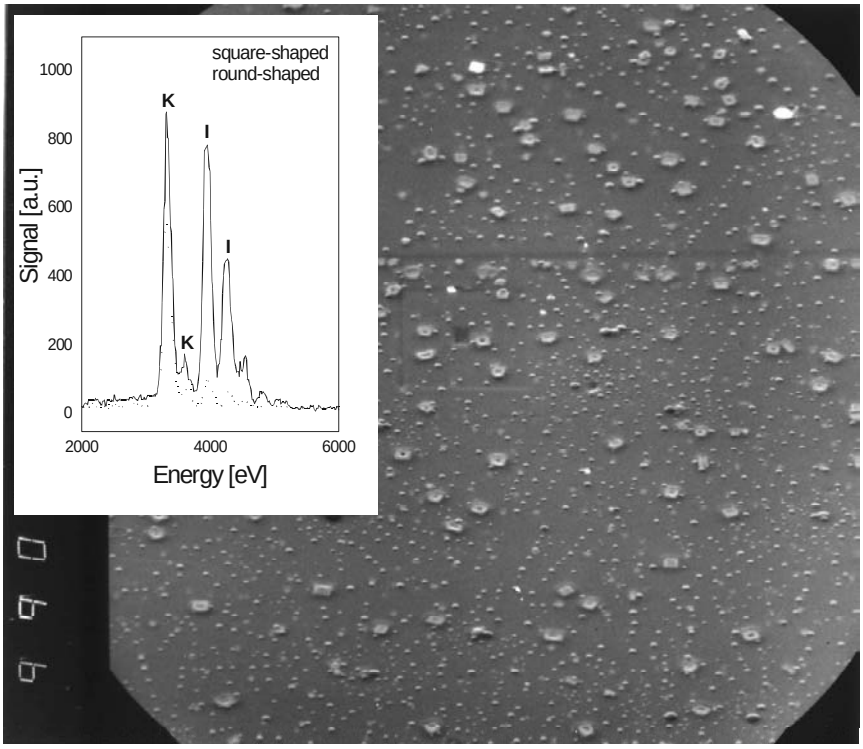

Figure 9. SEM micrograph of the microcrystallites that formed in the redox gel electrolyte catalysed with AcOH acid in a hybrid EC device cycled over 1830 cycles (100x magnification). Insert: EDX spectra of the squarish- and round-shaped microcrystallites.

The presence of KI microcrystallites we evidenced for the HEC device with the electrolyte catalysed with acetic acid (ICS-PPG/EtOH/KI/I_2/AcOH). This HEC device was opened and the redox electrolyte examined under an SEM microscope (Figure 9). Two kinds of defects were observed: squarish- and round-shaped crystallites. The dimensions of the larger crystallites were in the range 25 and 40 μm, the smaller between 1 to 5 μm. EDX measurements showed that the squarish crystallites corresponded to KI and the round-ones to potassium acetate. This was inferred from the EDX-analysis showing 50 at.% K and 50 at.% I for the squarish crystallites (Figure 9A) and 87 at.% of K and 13 at.% of I for the round crystallites (Figure 9B). The formation of the microcrystallites was undoubtedly connected to the evaporation of the volatile components, i.e. EtOH esters of AcOH or VaOH acids, from the electrolyte.

Reaction KI (microcrystallites) $\leftrightarrow$ KI_{1-x} + xK^+ + xI^- is consistent with the background changes in the HEC device (Figure 8). During the cathodic scan (0 V to –2 V) when the intercalation of K^+ ions in the WO_3 film took place, the KI microcrystallites dissociated, therefore diminished the concentration of the KI scattering centres and the background intensity decreased to minimal value (Figure 8C). After deintercalation of K^+ ions that was completed at approximately 1.3 V the intensity of the background increased again. Direct confirmation that the KI microcrystallites contributed to the background Raman scattering was obtained from in-situ Raman spectra measurements of a symmetric cell (not shown here). This cell was composed of two Pt-covered SnO_2:F-glass electrodes facing each other while the space between them was filled with the redox electrolyte. When the potential was changed in the same manner as shown in Figure 8A, no variation of the background intensity with potential was noted. This signalled that the concentration of the scattering centers, i.e. KI microcrystallites, did not change during the potential sweep. The reason for that lies in the fact that in the symmetric cell no WO_3 film is incorporated and the intercalation/deintercalation reaction of K^+ ions are therefore not possible. The concentration of KI microcrystallites, irrespective of their absolute initial concentration, did not change during the whole potential scanning of the symmetric cell.

The variations of the intensity of the $\nu_s(I_3^-)$ mode and the background followed the described pattern (Figure 8C) also when 32 CV cycles were measured successively (Figure 10). The cycling was performed with the scan rate of 5 mV s^{-1} and for each

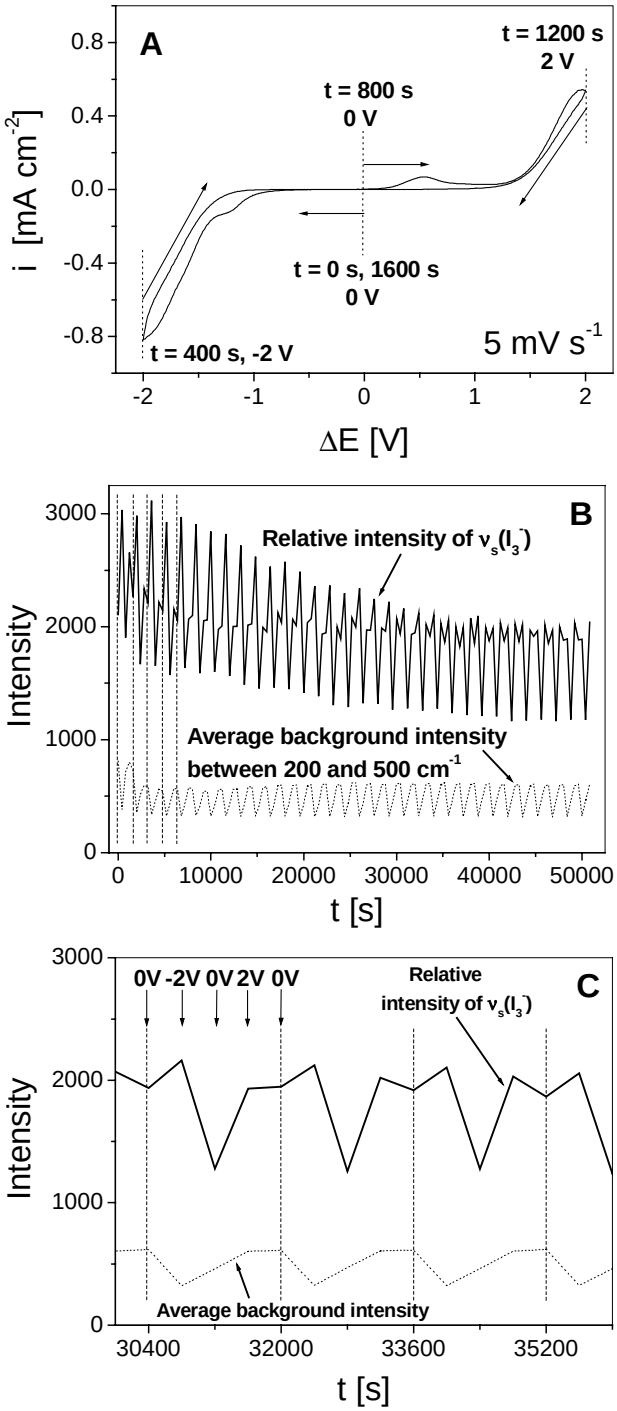

Figure 10. In-situ resonance Raman measurements (λ = 647.1 nm) of a hybird EC cell with electrolyte catalysed with VaOH: A) CV curve (12th cycle; 5 mV s^{-1}) and B,C) intensity changes of the $\nu_s(I_3^-)$ stretching mode and the background during CV cycling (32 cycles; dashed lines separate the cycles). In CV curve the arrows denote the starting potential and the duration (120 s) of the Raman measurement.

separate cycle four Raman spectra were recorded (every 400 s for 120 s) as shown by arrows in Figure 10. The higher intensity changes compared to those in Figure 8 can be explained by the longer time used for collection of the Raman spectra (120 s vs. 30 s) in the case of continuous measurement (Figure 10). In addition, the intensity vs. time plot showed that the intensity of the I_3^- stretching band decreased during the initial cycles, but then became more stabilised. This signified that the HEC cell needed some pre-cycling until a persistent electrochromic response developed. However, due to the inherent instability of the sol-gel redox electrolytes a small fading remained throughout the whole cycling of the device (more then 1000 cycles).

Conclusions

The hybrid EC device with gel redox electrolyte catalysed with valeric acid revealed quick colouring/bleaching performance. Most of the colouring was achieved in 20 s, while bleaching was even faster (5 s). The reason is that the HEC devices do not need the counter-electrode with the intercalation properties and therefore the kinetics of the coloration and bleaching, as well as the coloration efficiency, depends solely on the active electrochromic WO_3 film. The counter-electrode is in HEC devices platinised SnO_2:F-glass and the second redox pair is present in the gel redox electrolyte. The HEC device was characterised by the self-erasing effect contrary to the battery-type of the EC devices, which are due to their memory effect appropriate for the "smart windows" applications. Main application area of HEC devices is "rear-windows for cars" and important is that also reflective HEC devices can be prepared, simply by changing the thickness of the Pt-layer on the SnO_2:F-glass substrate.

The main emphasis in the present work was on in-situ resonance Raman spectroelectrochemical measurements. The resonance Raman spectra were found an excellent tool to follow the variation in the intensity of the symmetric $\nu_s(I_3^-)$ stretching at 111 cm^{-1}. These intensity changes directly reflected the course of the redox reaction $3I^- \leftrightarrow I_3^- + 2e^-$ closer to the Pt-side of the HEC device where we measured. At the same time we noted also the changes in the background intensities that were ascribed to dissociation/association of the KI microcrystallites in the gel redox electrolyte matrix. The presence of KI in the electrolyte is related to the evaporation of the volatile species as EtOH and ester of valeric acid from the sol-gel network during its ageing and was proved by SEM and EDX analysis.

Acknowledgements

The authors wish to thank the Ministry for Education, Science and Sport of the Republic of Slovenia for financial support under Programme P-506 and project J1-2125. Special thanks to Helena Spreizer, National Institute of Chemistry, for her technical assistance. Thanks also to Dr. Andreas Georg for the Pt covered glass electrodes. The paper was presented at the 13nd International "Symposium Spectroscopy in Theory and Practice" in Nova Gorica, Slovenia, 27 – 30 August, 2003.

References

1. R. D. Rauh, *Electrochim. Acta* **1999**, *44*, 3165–3176.
2. C. G. Granqvist, *Handbook of Inorganic Electrochromic Materials*; Elsevier Science, Amsterdam, 1995.
3. U. Opara Krašovec, A. Šurca Vuk, B. Orel, *Solar Energy Mater. Sol. Cells* **2002**, *73*, 21–37.
4. A. Šurca, B. Orel, B. Pihlar, P. Bukovec, *J. Electroanal. Chem.* **1996**, *408*, 83–100.
5. R. J. Mortimer, *Electrochim. Acta* **1999**, *44*, 2971–2981.
6. R. Cinnsealach, G. Boschloo, S. N. Rao, D. Fitzmaurice, *Solar Energy Mater. Sol. Cells* **1998**, *55*, 215–223.
7. R. Cinnsealach, G. Boschloo, S. N. Rao, D. Fitzmaurice, *Solar Energy Mater. Sol. Cells* **1999**, *57*, 107–125.
8. M.-A. de Paoli, G. Casalbore-Miceli, E. M. Girotto, W. A. Gazotti, *Electrochim. Acta* **1999**, *44*, 2983–2991.
9. P. M. S. Mond, R. J. Mortimer, D. R. Rosseinsky, *Electrochromism*; VCH, Weinheim, 1995.
10. C. F. Lin, C. L. Lin, L. C. Chen, K. C. Ho, 3rd ABA International Conference, June 16–20, 2002. Abstracts, Advanced Batteries and Accumulators – 3rd, University of Technology Brno, Faculty of Electrical Engineering and Communication, Brno, 2002, pp. 16–1.
11. U. Opara Krašovec, R. Ješe, B. Orel, J. Grdadolnik, G. Dražič, *Monatshefte für Chemie* **2002**, *133*, 1115–1133.
12. A. Šurca Vuk, B. Orel, H. Spreizer, Ph. Colomban, *Solid State Ionics* (in press).
13. A. Šurca Vuk, M. Gaberščck, B. Orel, Ph. Colomban, accepted to *J. Electrochem. Soc.*
14. U. Lavrenčič Štangar, B. Orel, N. Grošelj, Ph. Colomban, E. Stathatos, P. Lianos, *J. New Mater. Electrochem. Syst.* **2002**, *5*, 223–231.
15. B. Orel, U. Lavrenčič Štangar, A. Šurca Vuk, L. Panagiotis, Ph. Colomban, *Mat. Res. Soc. Symp. Proc*, **2002**, *730*, 273–278.
16. U. Lavrenčič Štangar, B. Orel, A. Šurca Vuk, G. Sagon, Ph. Colomban, E. Stathatos, P. Lianos, *J. Electrochem. Soc.* **2002**, *149*, E413–E423.
17. P. Judeinstein, C. Sanchez, *J. Mater. Chem.* **1996**, *6*, 511–525.
18. K. Damouche, M. Atik, N. C. Mello, T. J. Bonagamba, H. Penepucci, M. Aegerter, P. Judeinstein, *J. Sol-Gel Sci. Techn*. **1997**, *8*, 711−715.
19. U. Lavrenčič Štangar, B. Orel, B. Neuman, E. Stathatos, P. Lianos, *J. Sol-Gel Sci. Technol*. **2003**, *26*, 1113–1118.
20. H. Greijer, J. Lindgren, A. Hagfeld, *J. Phys. Chem. B* **2001**, *105*, 6314–6320.
21. A. Vioux, D. Leclerq, *Heterogen. Chem. Rev* **1996**, *3*, 1665–1671.
22. B. Orel, R. Ješe, U. Lavrenčič Štangar, J. Grdadolnik, M. Puchberger, submitted to *J. Non-Crystalline Solids*.
23. G. Wyszecki, W. S. Stiles, *Color Science*, 2nd Edition; Wiley, New York, 1982.
24. Z. Kebede, S.-E. Lindquist, *Solar Energy Mater. Sol. Cells* **1999**, *57*, 259–275.
25. P. Klaboe, *J. Am. Chem. Soc.* **1967**, *89*, 3667–3676.

26. W. Kiefer, H. J. Bernstein, *Chem. Phys. Lett.* **1972**, *16*, 5–9.
27. K. Kaya, N. Mikami, Y. Udagawa, M. Ito, *Chem. Phys. Lett.* **1972**, *16*, 151–153.
28. E. M. Nour, L. H. Chen, J. Laane, *J. Phys. Chem.* **1986**, *90*, 2841–2846.
29. J. Chaker, K. Dahmouche, V. Broiois, C. V. Santilli, S. H. Pulcinelli, P. Judeinstein, *J. Sol-Gel Sci. Technol.* **2003**, *26*, 1075–1080.

Povzetek

Hibriden elektrokromeni sklop smo pripravili iz optično aktivne tanke plasti WO_3 in SnO_2:F stekla z nanosom platine. Redoks elektrolit smo pripravili po sol-gel postopku iz organsko-anorganske prekurzorja ICS-PPG. Kot vir I_3^-/I^- redoks para smo uporabili KI in I_2 v molskem razmerju KI:I_2 = 10:1, kot katalizator pa valerinsko kislino. Stabilnost sklopa in hitrost obarvanja oz. razbarvanja smo določili z in-situ UV-vidnimi spektroelektrokemijskimi meritvami med +2 in –2 V. Z in-situ mikro Ramansko spektroskopijo smo zasledovali delovanje hibridnega sklopa. Svetlobo z valovno dolžino 647.1 nm smo usmerili v elektrolit v bližino Pt-elektrode in nato snemali Ramanske spektre med spreminjanjem potenciala s ciklovoltametrično elektrokemijsko tehniko. V Ramanskih spektrih je bil najbolj izražen trak simetričnega valenčnega nihanja I_3^- ionov. Na osnovi sprememb relativne intenzitete tega traku smo sklepali na potek reakcije $3I^- \leftrightarrow I_3^- + 2e^-$ v elektrolitu. V Ramanskih spektrih smo opazili tudi spremembe intenzitete ozadja, ki smo jih pripisali disociaciji/asociaciji KI mikrokristalitov v redoks elektrolitu med interkalacijo in deinterkalacijo K^+ ionov v elektrokromno tanko plast WO_3.